Inorganic Chemistry
Article

Inorg. Chem. **2010**, *49*, 9049–9054 **9049**
DOI: 10.1021/ic101461w

Arsenic-Containing Chalcophosphate Molecular Anions

Collin D. Morris and Mercouri G. Kanatzidis*

Department of Chemistry, Northwestern University, Evanston, Illinois 60208

Received July 21, 2010

We report five new discrete molecular arsenic-based chalcophosphates, $K_7As_3(P_2Se_6)_4$ (**1**), $K_6As_2(P_2Se_6)_3$ (**2**), $Cs_6As_2(P_2Se_6)_3$ (**3**), and $Cs_5As(P_2Q_6)_2$ [Q = Se (**4a**) and S (**4b**)]. Each of the compounds contains unique complex anions comprised of common building blocks that have condensed to produce these anions. Phosphorus forms well-known $[P_2Q_6]^{4-}$ moieties in all of the compounds that are bridged by arsenic trigonal pyramids in **1** and **2** and distorted octahedra in **3**, **4a**, and **4b**. Although **2** and **3** have the same molecular formula, the structural difference between the two salts is attributed to the size of the alkali metal. The influence of flux basicity also seems to play a role in the formation of the molecular anion in **4a** and **4b**, which has been observed with other trivalent main-group elements at the octahedral position but only with the highly basic cesium alkali metal as the counterion. All structures were determined by single-crystal X-ray diffraction and are discussed along with phase-purity powder X-ray diffraction, thermal analyses, electronic absorption, and Raman spectroscopy.

Introduction

Exploratory synthesis in the area of alkali-metal chalcophosphates and chalcoarsenates has resulted in the discovery of a variety of different complex anions and structures.[1−4] These unique $[Pn_yQ_z]^{n-}$ (Pn = P, As; Q = S, Se) anions have been stabilized primarily by using the polychalcogenide molten flux method, which allows complex and diverse phases to form by exploiting the low melting point (200−600 °C) and oxidative properties of the $A_xPn_yQ_z$ flux (A = alkali metal).[4] The complexity observed among such anions ranges from discrete molecular species to one-dimensional, polymeric chains and includes $[PnQ_4]^{3-}$,[5−8] $[P_2Q_6]^{4-}$,[9,10] $[P_2Se_9]^{4-}$,[5,11] $[P_8Se_{18}]^{6-}$,[12] $[AsS_3]^{3-}$,[13] β-$[AsS_4]^{3-}$,[3] and the $^1/_\infty[PSe_6^-]$,[14] $^1/_\infty[P_5Se_{10}^{5-}]$,[15] and $^1/_\infty[AsQ_2^-]$[16−18] infinite polymers. These compounds are generally wide-gap semiconductors that exhibit technologically relevant properties such as second-harmonic generation,[2,17−20] ferroelectricity,[21−23] photoluminescence[24,25] and reversible phase-change transitions.[20,25,26]

Further structural diversity is found in quaternary chalcophosphates and chalcoarsenates containing a transition-metal or main-group element.[2,24,27,28] In the latter compounds,

*To whom correspondence should be addressed. E-mail: m-kanatzidis@northwestern.edu.

(1) (a) Kanatzidis, M. G.; Sutorik, A. C. *Prog. Inorg. Chem.* **1995**, *43*, 151. (b) Liao, J. H.; Varotsis, C.; Kanatzidis, M. G. *Inorg. Chem.* **1993**, *32*, 2453–2462. (c) Park, Y. B.; Kanatzidis, M. G. *Angew. Chem., Int. Ed. Engl.* **1990**, *29*, 914–915.
(2) Bera, T. K.; Jang, J. I.; Ketterson, J. B.; Kanatzidis, M. G. *J. Am. Chem. Soc.* **2009**, *131*, 75.
(3) Iyer, R. G.; Kanatzidis, M. G. *Inorg. Chem.* **2002**, *41*, 3605.
(4) Kanatzidis, M. G. *Curr. Opin. Solid State Mater. Sci.* **1997**, *2*, 139.
(5) (a) Knaust, J. M.; Dorhout, P. K. *J. Chem. Crystallogr.* **2006**, *36*, 217. (b) Kanatzidis, M. G.; Huang, S. P. *Inorg. Chem.* **1989**, *28*, 4667–4669. (c) Kanatzidis, M. G.; Park, Y. *Chem. Mater.* **1990**, *2*, 99–101.
(6) Garin, J.; Parthe, E. *Acta Crystallogr., Sect. B* **1972**, *28*, 3672.
(7) Chondroudis, K.; Hanko, J. A.; Kanatzidis, M. G. *Inorg. Chem.* **1997**, *36*, 2623.
(8) Bera Tarun, K.; Iyer Ratnasabapathy, G.; Malliakas Christos, D.; Kanatzidis Mercouri, G. *Inorg. Chem.* **2007**, *46*, 8466.
(9) McCarthy, T. J.; Kanatzidis, M. G. *J. Chem. Soc., Chem. Commun.* **1994**, 1089.
(10) Chondroudis, K.; McCarthy, T. J.; Kanatzidis, M. G. *Inorg. Chem.* **1996**, *35*, 3451.
(11) Chondroudis, K.; Kanatzidis, M. G. *Inorg. Chem.* **1995**, *34*, 5401.
(12) Chondroudis, K.; Kanatzidis, M. G. *Inorg. Chem.* **1998**, *37*, 2582.
(13) Bera Tarun, K.; Kanatzidis Mercouri, G. *Inorg. Chem.* **2008**, *47*, 7068.
(14) Chung, I.; Do, J.; Canlas, C. G.; Weliky, D. P.; Kanatzidis, M. G. *Inorg. Chem.* **2004**, *43*, 2762.
(15) Chondroudis, K.; Kanatzidis, M. G. *Angew. Chem., Int. Ed. Engl.* **1997**, *36*, 1324.
(16) Palazzi, M.; Jaulmes, S. *Acta Crystallogr., Sect. B* **1977**, *B33*, 908.
(17) Bera, T. K.; Song, J.-H.; Freeman, A. J.; Jang, J. I.; Ketterson, J. B.; Kanatzidis, M. G. *Angew. Chem., Int. Ed.* **2008**, *47*, 7828.
(18) Bera, T. K.; Jang, J. I.; Song, J.-H.; Malliakas, C. D.; Freeman, A. J.; Ketterson, J. B.; Kanatzidis, M. G. *J. Am. Chem. Soc.* **2010**, *132*, 3484.
(19) Chung, I.; Song, J.-H.; Jang, J. I.; Freeman, A. J.; Ketterson, J. B.; Kanatzidis, M. G. *J. Am. Chem. Soc.* **2009**, *131*, 2647.
(20) Chung, I.; Jang, J.-I.; Malliakas, C. D.; Ketterson, J. B.; Kanatzidis, M. G. *J. Am. Chem. Soc.* **2010**, *132*, 384.
(21) Carpentier, C. D.; Nitsche, R. *Mater. Res. Bull.* **1974**, *9*, 1097.
(22) Rogach, E. D.; Sviridov, E. V.; Arnautova, E. A.; Savchenko, E. A.; Protsenko, N. P. *Zh. Tekh. Fiz.* **1991**, *61*, 201.
(23) Scott, B.; Pressprich, M.; Willet, R. D.; Cleary, D. A. *J. Solid State Chem.* **1992**, *96*, 294.
(24) Banerjee, S.; Malliakas, C. D.; Jang, J. I.; Ketterson, J. B.; Kanatzidis, M. G. *J. Am. Chem. Soc.* **2008**, *130*, 12270.
(25) Chung, I.; Song, J.-H.; Kim, M. G.; Malliakas, C. D.; Karst, A. L.; Freeman, A. J.; Weliky, D. P.; Kanatzidis, M. G. *J. Am. Chem. Soc.* **2009**, *131*, 16303.
(26) Chung, I.; Jang, J. I.; Gave, M. A.; Weliky, D. P.; Kanatzidis, M. G. *Chem. Commun.* (*Cambridge, U.K.*) **2007**, 4998.
(27) Rothenberger, A.; Wang, H. H.; Chung, D.; Kanatzidis, M. G. *Inorg. Chem.* **2010**, *49*, 1144.

Published on Web 09/08/2010

the heavier group 15 congeners such as bismuth and antimony, with their large ionic radii and flexible coordination spheres, serve to further link the chalcogenide building blocks and form new structures.[29−32] Compounds in which the chalcogen atoms are mixed have also been synthesized.[27] Generally, these structures are described as having mixed occupancy between sulfur and selenium on the chalcogen sites, although slight preferences at specific sites have been observed.[28,33] Despite these findings, synthesis of structures containing phosphorus and arsenic have been much less explored.[34,35] In fact, no compounds comprised of A/As/P/Q have been reported. In part because of the stereochemically active lone pair typically expressed by arsenic, the oxidation state and local coordination environment of the two pnicogens tends to be different. Therefore, structures with pnicogen specific sites should be expected. Herein, we report the successful synthesis of the first arsenic-containing chalcophosphates. These compounds are molecular salts and feature common As and P units that have condensed to form complex anions.

Experimental Section

Reagents. All reagents were used as obtained: potassium metal (98%, Sigma Aldrich, St. Louis, MO); cesium metal (99.9+%, Strem Chemicals, Inc., Newburyport, MA); arsenic powder (99%, Alfa Aesar, Ward Hill, MA); red phosphorus powder (99%, Sigma Aldrich, St. Louis, MO); selenium pellets (99.99%, Sigma Aldrich, St. Louis, MO); sulfur powder (99.98%, Sigma Aldrich, St. Louis, MO); *N*,*N*′-dimethylformamide (DMF; ACS grade, Mallinckrodt Chemical, Phillipsburg, NJ); diethyl ether (ACS grade, BDH Chemicals, Leicestershire, U.K.). K_2Se, Cs_2Se_2, and Cs_2S were prepared by reacting stoichiometric amounts of the elements in liquid ammonia as described elsewhere.[36,37]

Synthesis. All compounds were synthesized by adding the correct stoichiometric amounts of alkali-metal chalcogenide (K_2Se, Cs_2Se_2, or Cs_2S), phosphorus, arsenic, and Q to a 9-mm fused-silica tube in a N_2-filled glovebox. The tubes were sealed under vacuum ($< 10^{-4}$ mbar), heated to 500 °C over the course of 6 h, and reacted at this temperature for 3 days. The tubes were then cooled to 200 °C over 60 h, at which point the furnace was turned off and the tubes were allowed to cool to room temperature in ∼3 h. The products were washed with degassed DMF and dried with diethyl ether in a N_2 atmosphere to give the desired product.

$K_7As_3(P_2Se_6)_4$ (1). A mixture of 63 mg (0.40 mmol) of K_2Se, 26 mg (0.35 mmol) of arsenic, 28 mg (0.90 mmol) of phosphorus, and 184 mg (2.33 mmol) of selenium was added to a 9-mm fused-silica tube, sealed under vacuum, and subjected to the specified heating profile. After washing with DMF for 2 days, red crystals of **1** were achieved in 38% yield.

$K_6As_2(P_2Se_6)_3$ (2). A mixture of 71 mg (0.45 mmol) of K_2Se, 23 mg (0.31 mmol) of arsenic, 28 mg (0.90 mmol) of phosphorus, and 178 mg (2.25 mmol) of selenium was added to a 9-mm fused-silica tube, sealed under vacuum, and subjected to the specified heating profile. After washing with DMF for 2 days, orange crystals of **2** were achieved in 15% yield.

$Cs_6As_2(P_2Se_6)_3$ (3). A mixture of 149 mg (0.35 mmol) of Cs_2Se_2, 18 mg (0.24 mmol) of arsenic, 22 mg (0.71 mmol) of phosphorus, and 111 mg (1.41 mmol) of selenium was added to a 9-mm fused-silica tube, sealed under vacuum, and subjected to the specified heating profile. After washing with DMF for 2 days, orange crystals of **3** were achieved in 78% yield.

$Cs_5As(P_2Se_6)_2$ (4a). A mixture of 176 mg (0.42 mmol) of Cs_2Se_2, 12 mg (0.16 mmol) of arsenic, 21 mg (0.68 mmol) of phosphorus, and 92 mg (1.17 mmol) of selenium was added to a 9-mm fused-silica tube, sealed under vacuum, and subjected to the specified heating profile. After washing with DMF for 2 days, red crystals of **4a** were achieved in 61% yield.

$Cs_5As(P_2S_6)_2$ (4b). A mixture of 179 mg (0.60 mmol) of Cs_2S, 18 mg (0.24 mmol) of arsenic, 30 mg (0.97 mmol) of phosphorus, and 73 mg (2.28 mmol) of sulfur was added to a 9-mm fused-silica tube, sealed under vacuum, and subjected to the specified heating profile. After washing with degassed DMF for 6 h, yellow crystals of **4b** were achieved in 40% yield.

Powder X-ray Diffraction (PXRD). Phase-purity powder X-ray diffraction analyses were performed using a silicon-calibrated CPS 120 INEL powder X-ray diffractometer (Cu Kα graphite-monochromatized radiation) operating at 40 kV and 20 mA, equipped with a position-sensitive detector with a flat sample geometry. Simulated patterns were generated using the *Visualizer* program of FindIt and the CIF of each refined structure.

Scanning Electron Microscopy (SEM). Semiquantitative microprobe analyses and energy-dispersive spectroscopy (EDS) were performed with a Hitachi S-3400 scanning electron microscope equipped with a PGT energy-dispersive X-ray analyzer. Data were acquired with an accelerating voltage of 25 kV and a 60 s accumulation time.

Solid-State UV−vis Spectroscopy. Optical diffuse-reflectance measurements were performed at room temperature using a Shimadzu UV-3101 PC double-beam, double-monochromator spectrophotometer operating from 200 to 2500 nm. The instrument was equipped with an integrating sphere and controlled by a personal computer. $BaSO_4$ was used as a 100% reflectance standard. The sample was prepared by grinding the crystals to a powder, which was then spread on a compacted bed of $BaSO_4$ powder. The generated reflectance-versus-wavelength data were used to estimate the band gap of the material by converting reflectance to absorbance data according to the Kubelka−Munk equation: $\alpha/S = (1 - R)^2/2R$, where R is the reflectance and α and S are the absorption and scattering coefficients, respectively.[38]

Differential Thermal Analysis (DTA). DTA experiments were performed on a Shimadzu DTA-50 thermal analyzer. A sample (∼40 mg) of ground crystalline material was sealed in a fused-silica ampule under vacuum. A similar ampule filled with an equal mass of Al_2O_3 was sealed and used as a reference. The melting and crystallization points were measured at the onset of the endothermic and exothermic peaks, respectively.

Single-Crystal X-ray Crystallography. Single-crystal X-ray diffraction experiments were performed using either a STOE IPDS II or IPDS 2T diffractometer using Mo Kα radiation (λ = 0.710 73 Å) and operating at 50 kV and 40 mA. Integration and numerical absorption corrections were performed using the

(28) Rothenberger, A.; Morris, C.; Wang, H. H.; Chung, D. Y.; Kanatzidis, M. G. *Inorg. Chem.* **2009**, *48*, 9036.
(29) McCarthy, T. J.; Kanatzidis, M. G. *Chem. Mater.* **1993**, *5*, 1061.
(30) McCarthy, T. J.; Ngeyi, S. P.; Liao, J. H.; DeGroot, D. C.; Hogan, T.; Kannewurf, C. R.; Kanatzidis, M. G. *Chem. Mater.* **1993**, *5*, 331.
(31) McCarthy, T. J.; Hogan, T.; Kannewurf, C. R.; Kanatzidis, M. G. *Chem. Mater.* **1994**, *6*, 1072.
(32) Yao, J.; Deng, B.; Ellis, D. E.; Ibers, J. A. *Inorg. Chem.* **2002**, *41*, 7094.
(33) Kyratsi, T.; Dyck, J. S.; Chen, W.; Chung, D. Y.; Uher, C.; Paraskevopoulos, K. M.; Kanatzidis, M. G. *Mater. Res. Soc. Symp. P* **2001**, *691*, 419.
(34) Hoenle, W.; Wibbelmann, C.; Brockner, W. *Z. Naturforsch., B: Anorg. Chem., Org. Chem.* **1984**, *39B*, 1088.
(35) Christian, B. H.; Gillespie, R. J.; Sawyer, J. F. *Acta Crystallogr., Sect. C: Cryst. Struct. Commun.* **1987**, *C43*, 187.
(36) McCarthy, T. J.; Ngeyi, S. P.; Liao, J. H.; Degroot, D. C.; Hogan, T.; Kannewurf, C. R.; Kanatzidis, M. G. *Chem. Mater.* **1993**, *5*, 331.
(37) McCarthy, T. J.; Kanatzidis, M. G. *Inorg. Chem.* **1995**, *34*, 1257.
(38) (a) Kortum, G.; Braun, W.; Herzog, G. *Angew. Chem.* **1963**, *75*, 653. (b) Larson, P.; Mahanti, S. D.; Kanatzidis, M. G. *Physical Review B* **2000**, *61*, 8162. (c) McCarthy, T. J.; Tanzer, T. A.; Kanatzidis, M. G. *J. Am. Chem. Soc.* **1995**, *117*, 1294. (d) Trikalitis, P. N.; Rangan, K. K.; Bakas, T.; Kanatzidis, M. G. *J. Am. Chem. Soc.* **2002**, *124*, 12255.

Table 1. Crystallographic Refinement Details for Reported Compounds

	1	2	3	4a	4b
formula	$K_7As_3(P_2Se_6)_4$	$K_6As_2(P_2Se_6)_3$	$Cs_6As_2(P_2Se_6)_3$	$Cs_5As(P_2Se_6)_2$	$Cs_5As(P_2S_6)_2$
fw	2641.26	1991.54	2554.40	1810.87	1248.07
λ, Å	0.710 73	0.710 73	0.710 73	0.710 73	0.710 73
temperature, K	100(2)	100(2)	100(2)	100(2)	293(2)
cryst syst	monoclinic	monoclinic	monoclinic	tetragonal	tetragonal
space group	$P2_1/c$	$P2_1/c$	$P2_1/c$	$P4_2/m$	$P4_2/m$
a, Å	25.0706(3)	8.0898(5)	19.576(2)	13.8260(8)	13.5875(8)
b, Å	9.5948(1)	23.314(2)	7.9206(6)	13.8260(8)	13.5875(8)
c, Å	59.6227(9)	12.1919(7)	13.0553(9)	7.5173(4)	7.2999(4)
α, deg	90	90	90	90	90
β, deg	93.384(1)	124.809(4)	101.914(6)	90	90
γ, deg	90	90	90	90	90
V, Å^3	14317.0(4)	1888.0(2)	1980.7(3)	1437.0(2)	1347.7(1)
Z	12	2	2	2	2
ρ, mg/m^3	3.676	3.503	4.283	4.185	3.076
μ, mm^{-1}	21.283	20.040	23.907	22.837	9.074
$F(000)$	14016	1764	2196	1552	1120
θ_{max}, deg	25.00	29.33	29.12	29.15	29.10
reflns collected	68 995	15 753	16 260	10 986	9423
unique reflns	24207	5057	5065	2060	1928
R_{int}, %	13.13	6.78	8.37	7.31	5.62
no. of param	1135	145	145	65	64
refinement method	full-matrix least squares on F^2				
GOF	0.981	1.108	0.962	1.429	1.191
final R indices [$I > 2\sigma(I)$], R1[a]/wR2[b], %	5.91/14.09	6.34/8.74	5.46/14.08	6.43/14.17	6.23/13.88
R indices (all data), R1/wR2, %	9.25/16.08	10.43/9.59	7.23/15.10	6.62/14.23	6.66/14.06

[a] $R1 = \sum||F_o| - |F_c||/\sum|F_o|$. [b] $wR2 = \{\sum[w(F_o^2 - F_c^2)^2]/\sum[w(F_o^2)^2]\}^{1/2}$.

X-AREA, *X-RED*, and *X-SHAPE* programs. Each structure was solved by direct methods and refined by full-matrix least squares on F^2 using the *SHELXTL* program package.[39] For $Cs_5As(P_2Q_6)_2$, a twin law of 180° rotation down the a axis (1 0 0 0 −1 0 0 0 −1) was suggested by TwinRotMat in the *PLATON*[40] suite of programs and applied with refined BASF parameters of 0.19 and 0.27 for **4a** and **4b**, respectively.

Raman Spectroscopy. Raman spectra for pure compounds were collected on a DeltaNu Advantage NIR spectrometer using 785 nm radiation from a diode laser equipped with a CCD camera detector. A max power of 60 mW and a beam diameter of 35 μm were used. The spectra were collected on ground crystalline samples using an integration time of 5 s.

Results and Discussion

Five new discrete molecular arsenic-containing chalcophosphates have been synthesized using the polychalcogenide flux method. Dark-red single crystals of **1** were initially synthesized in a low-basicity flux (K:Se = 1:4.5) using K_2Se, P_2Se_5, and As_2Se_3. Semiquantitative EDS analysis of several crystals indicated the presence of all elements with values close to those determined from the structure solution (Figure S1 in the Supporting Information). **1** crystallizes in the monoclinic space group $P2_1/c$ with an unusually long c axis of 59.699(2) Å (Table 1). The new $[As_3(P_2Se_6)_4]^{7-}$ anion contains four ethane-like $[P_2Se_6]^{4-}$ units bridged by three As^{3+} ions that are each in a trigonal-pyramidal environment. This complex anion wraps around on itself in a complicated manner and is stabilized by short intra- and intermolecular nonbonding Se···Se interactions ranging from 3.442(4) to 3.649(4) Å (Figure 1). A modified synthesis using K_2Se, phosphorus, arsenic, and selenium in the correct stoichiometric amounts was performed in an attempt to obtain the product as a pure phase; however, several orange crystals were observed along with a majority of red crystals. The red and orange products are **1** and the new compound **2**, respectively. Further attempts to synthesize a pure compound proved to be unsuccessful. Diffuse-reflectance UV−vis spectroscopy seems to indicate that a pure phase was obtained with a band gap of 2.0 eV, which is consistent with the red crystals of **1**, but PXRD and DTA show evidence of the impurity (Figures 2 and S2 and S3 in the Supporting Information). **1** melts congruently at 388 °C and shows a weak exothermic peak, indicating crystallization at 361 °C. The melting and crystallization points of the impurity, **2**, can be seen at 405 and 392 °C, respectively, and are relatively unchanged from those determined for the pure compound, discussed below.

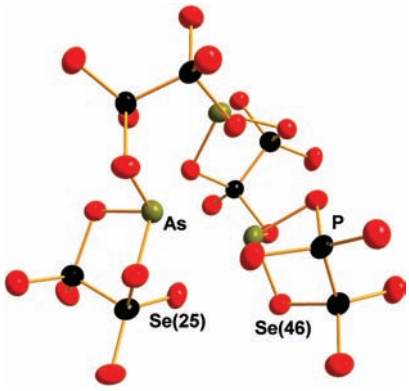

Figure 1. Single molecular anionic unit of **1** with thermal ellipsoids set at 90%. Each discrete molecule contains four P_2Se_6 units bridged by trigonal-pyramidal As ions. The intramolecular nonbonding Se(25)···Se(46) interaction shown is 3.543(4) Å.

$K_6As_2(P_2Se_6)_3$ also crystallizes in $P2_1/c$ and is related to the previously reported compound $K_6P_8Se_{18}$.[12] Both compounds form a pseudolinear arrangement of three $[P_2Se_6]^{4-}$ anions bridged by two pnicogen trigonal pyramids that are oriented in opposite directions (Figure 3). The discrete anions in **2**

(39) Sheldrick, G. M. *Acta Crystallogr., Sect. A* **2008**, *64*, 112.
(40) Spek, A. L. *J. Appl. Crystallogr.* **2003**, *36*, 7.

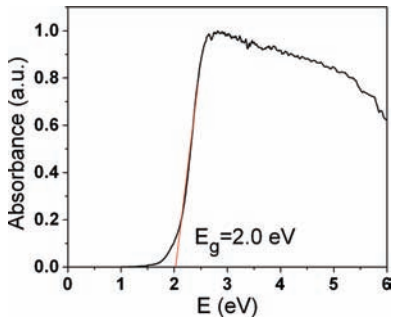

Figure 2. Solid-state UV−vis spectrum of **1**. The sharp absorption seems to indicate that a pure phase has been synthesized, but **2** is present as a minor impurity.

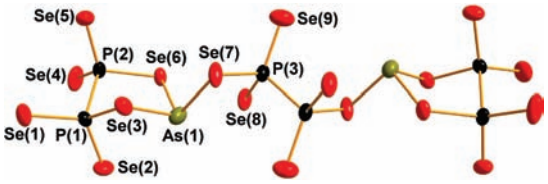

Figure 3. Discrete anionic unit of **2** with thermal ellipsoids set at 60%. The $AsSe_3$ trigonal pyramids are oriented in opposite directions and bridge neighboring P_2Se_6 units. A center of inversion is located at the midpoint of the P(3)−P(3) bond.

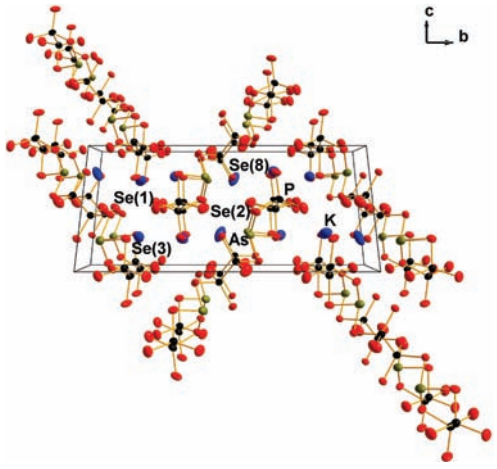

Figure 4. Expanded unit cell of **2** viewed down the *a* axis. Thermal ellipsoids are set at 70%. The discrete anions stack on top of one another to form columns that pack in the *bc* plane with short, nonbonding Se···Se interactions. Selected distances (Å): Se(2)−Se(8), 3.631(2); Se(1)−Se(3), 3.78(2).

stack directly on top of one another along the *a* axis to form a columnar topology, which is slightly different from the step-like packing of the anions in $K_6P_8Se_{18}$. Short, nonbonding Se···Se interactions [3.631(2) and 3.78(2) Å] also influence the packing of the anions in the *bc* plane (Figure 4). With the stoichiometry determined by the structure solution and verified by EDS analysis, a reaction of K_2Se, phosphorus, arsenic, and selenium in the proper ratios resulted in **2** as a pure phase (Figures S4 and S5 in the Supporting Information). **2** exhibits a sharp band-gap transition at 2.2 eV, consistent with its orange color, and melts congruently at 410 °C (Figures S6 and S7 in the Supporting Information). The Raman spectrum of **2** shows many peaks characteristic of the $[P_2Se_6]^{4-}$ anion, most notably the strongest at 222 cm^{-1}, which is indicative of the totally symmetric stretching vibration

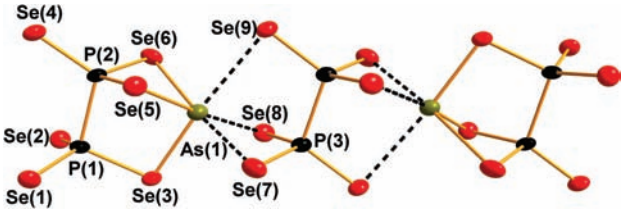

Figure 5. Discrete anionic unit of **3** with thermal ellipsoids set at 90%. Short, nonbonding As···Se interactions are indicated by dashed bonds. A center of inversion is located at the midpoint of the P(3)−P(3) bond. Selected distances (Å): As(1)−Se(3), 2.483(1); As(1)−Se(5), 2.563(1); As(1)−Se(6), 2.685(1); As(1)−Se(7), 2.710(1), As(1)−Se(8), 2.854(1); As(1)−Se(9), 3.186(1).

Table 2. Selected Bond Lengths (Å) and Angles (deg) for **2** at 100(2) K[a]

As(1)−Se(7)	2.3863(13)	Se(2)−P(1)−P(2)	111.24(11)
As(1)−Se(6)	2.4084(13)	Se(1)−P(1)−Se(3)	109.16(10)
As(1)−Se(3)	2.4139(14)	Se(2)−P(1)−Se(3)	109.38(10)
P(1)−Se(1)	2.120(2)	P(2)−P(1)−Se(3)	98.87(9)
P(1)−Se(2)	2.140(2)	Se(9)−P(3)−Se(8)	121.18(12)
P(1)−P(2)	2.239(3)	Se(9)−P(3)−P(3)	111.15(14)
P(1)−Se(3)	2.258(2)	Se(8)−P(3)−P(3)	106.68(14)
P(3)−Se(9)	2.133(2)	Se(9)−P(3)−Se(7)	106.16(10)
P(3)−Se(8)	2.148(2)	Se(8)−P(3)−Se(7)	109.22(10)
P(3)−P(3)	2.235(4)	P(3)−P(3)−Se(7)	100.51(14)
P(3)−Se(7)	2.264(2)	Se(4)−P(2)−Se(5)	115.79(10)
P(2)−Se(4)	2.137(2)	Se(4)−P(2)−P(1)	108.11(11)
P(2)−Se(5)	2.137(2)	Se(5)−P(2)−P(1)	110.63(11)
P(2)−Se(6)	2.286(2)	Se(4)−P(2)−Se(6)	109.38(10)
Se(7)−As(1)−Se(6)	104.46(5)	Se(5)−P(2)−Se(6)	111.11(10)
Se(7)−As(1)−Se(3)	86.58(4)	P(1)−P(2)−Se(6)	100.74(10)
Se(6)−As(1)−Se(3)	100.68(4)	P(3)−Se(7)−As(1)	94.75(7)
Se(1)−P(1)−Se(2)	118.46(10)	P(1)−Se(3)−As(1)	89.57(6)
Se(1)−P(1)−P(2)	107.93(11)	P(2)−Se(6)−As(1)	101.65(6)

[a] Symmetry codes: (1) $x-1, y, z$; (2) $-x+1, y-{}^1/_2, -z+{}^1/_2$; (3) $x, -y+{}^1/_2, z-{}^1/_2$; (4) $-x, -y+1, -z$; (5) $x-1, -y+{}^1/_2, z-{}^1/_2$; (6) $x, -y+{}^1/_2, z+{}^1/_2$; (7) $x+1, y, z$; (8) $x+1, -y+{}^1/_2, z+{}^1/_2$; (9) $-x+1, y+{}^1/_2, -z+{}^1/_2$; (10) $-x+1, -y+1, -z+1$; (11) $-x+1, -y+1, -z$; (12) $-x, y+{}^1/_2, -z+{}^1/_2$; (13) $-x, y-{}^1/_2, -z+{}^1/_2$.

(Figure S8 in the Supporting Information). All others can be assigned as various stretches and bends of the anion.[41]

Attempts at making the cesium analogues of these compounds resulted in two new compounds, **3** and **4a**. Orange crystals of **3** were synthesized as a pure phase by the reaction of Cs_2Se_2, phosphorus, arsenic, and selenium in the proper stoichiometric ratios, and EDS indicates good agreement with the given stoichiometry (Figures S9 and S10 in the Supporting Information). **3** crystallizes in the same space group as its potassium analogue but contains a slightly different anion. Rather than bridging two $[P_2Se_6]^{4-}$ units, each of two As^{3+} ions is bound to one selenophosphate anion in a chelating-type interaction (Figure 5). This allows for short interactions [2.710(1)−2.854(1) Å] between the lone pair on As and two Se atoms [i.e., Se(7) and Se(5)] on the central selenophosphate unit, forming a distorted octahedron when the sixth Se atom at 3.186(1) Å is considered. Although the anions of **2** and **3** have a center of inversion at the midpoint of the P−P bond of the central P_2Se_6 moiety, the

(41) (a) Aitken, J. A.; Evain, M.; Iordanidis, L.; Kanatzidis, M. G. *Inorg. Chem.* **2002**, *41*, 180. (b) Chung, I.; Holmes, D.; Weliky, D. P.; Kanatzidis, M. G. *Inorg. Chem.* **2010**, *49*, 3092. (c) Chung, I.; Malliakas, C. D.; Jang, J. I.; Canlas, C. G.; Weliky, D. P.; Kanatzidis, M. G. *J. Am. Chem. Soc.* **2007**, *129*, 14996. (d) Hanko, J. A.; Sayettat, J.; Jobic, S.; Brec, R.; Kanatzidis, M. G. *Chem. Mater.* **1998**, *10*, 3040. (e) Rothenberger, A.; Morris, C.; Kanatzidis, M. G. *Inorg. Chem.* **2010**, *49*, 5598.

Table 3. Selected Bond Lengths (Å) and Angles (deg) for **3** at 100(2) K[a]

As(1)−Se(3)	2.4831(13)	Se(7)−As(1)−Se(8)	80.94(4)
As(1)−Se(5)	2.5636(13)	Se(2)−P(1)−Se(1)	119.50(11)
As(1)−Se(6)	2.6854(13)	Se(2)−P(1)−P(2)	106.33(11)
As(1)−Se(7)	2.7099(13)	Se(1)−P(1)−P(2)	107.10(11)
As(1)−Se(8)	2.8535(13)	Se(2)−P(1)−Se(3)	111.94(10)
As(1)−Se(9)	3.186(1)	Se(1)−P(1)−Se(3)	110.46(10)
P(1)−Se(2)	2.127(2)	P(2)−P(1)−Se(3)	99.31(11)
P(1)−Se(1)	2.129(2)	Se(4)−P(2)−Se(6)	117.02(10)
P(1)−P(2)	2.229(3)	Se(4)−P(2)−P(1)	110.66(12)
P(1)−Se(3)	2.293(2)	Se(6)−P(2)−P(1)	104.11(11)
P(2)−Se(4)	2.103(2)	Se(4)−P(2)−Se(5)	116.52(11)
P(2)−Se(6)	2.209(2)	Se(6)−P(2)−Se(5)	104.26(10)
P(2)−P(1)	2.229(3)	P(1)−P(2)−Se(5)	102.63(10)
P(2)−Se(5)	2.244(2)	Se(9)−P(3)−Se(8)	114.58(11)
P(3)−Se(9)	2.143(2)	Se(9)−P(3)−Se(7)	113.45(10)
P(3)−Se(8)	2.182(2)	Se(8)−P(3)−Se(7)	110.79(11)
P(3)−Se(7)	2.207(2)	Se(9)−P(3)−P(3)	108.69(15)
P(3)−P(3)	2.240(4)	Se(8)−P(3)−P(3)	105.51(14)
Se(1)−Se(2)	3.6758(12)	Se(7)−P(3)−P(3)	102.79(14)
Se(2)−Se(4)	3.8649(14)	P(1)−Se(1)−Se(2)	30.23(7)
Se(3)−As(1)−Se(5)	93.57(4)	P(1)−Se(2)−Se(1)	30.27(6)
Se(3)−As(1)−Se(6)	92.81(4)	P(1)−Se(2)−Se(4)	124.61(7)
Se(5)−As(1)−Se(6)	84.05(4)	Se(1)−Se(2)−Se(4)	95.15(3)
Se(3)−As(1)−Se(7)	92.14(4)	P(1)−Se(3)−As(1)	99.44(6)
Se(5)−As(1)−Se(7)	96.49(4)	P(2)−Se(4)−Se(2)	142.83(8)
Se(6)−As(1)−Se(7)	174.98(5)	P(2)−Se(5)−As(1)	79.08(7)
Se(3)−As(1)−Se(8)	91.90(4)	P(2)−Se(6)−As(1)	77.03(6)
Se(5)−As(1)−Se(8)	174.05(5)	P(3)−Se(7)−As(1)	79.95(7)
Se(6)−As(1)−Se(8)	98.03(4)	P(3)−Se(8)−As(1)	77.12(7)

[a] Symmetry codes: (1) $x, y+1, z$; (2) $-x+1, -y+1, -z+1$; (3) $x, -y+{}^3/_2, z-{}^1/_2$; (4) $-x, y+{}^1/_2, -z+{}^1/_2$; (5) $-x, y-{}^1/_2, -z+{}^1/_2$; (6) $x, -y+{}^1/_2, z-{}^1/_2$; (7) $x, -y+{}^1/_2, z+{}^1/_2$; (8) $-x+1, -y, -z+1$; (9) $-x+1, y-{}^1/_2, -z+{}^1/_2$; (10) $-x+1, -y, -z$; (11) $-x+1, y+{}^1/_2, -z+{}^1/_2$; (12) $x, y-1, z$; (13) $-x, -y, -z$; (14) $x, -y+{}^3/_2, z+{}^1/_2$.

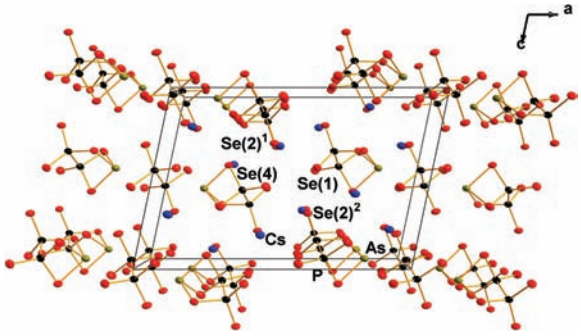

Figure 6. Expanded unit cell of **3** viewed down the *b* axis. Thermal ellipsoids are set at 90%. The larger Cs cations residing between the molecular anions push the neighboring P_2Se_6 units further away from one another, forcing As to coordinate in a chelate fashion to a single P_2Se_6 ligand. Selected distances (Å): $Se(1)-Se(2)^2$, 3.676(1); $Se(2)^1-Se(4)$, 3.790(1). Superscript symmetry codes: (1) $x, 1+y, z$; (2) $1-x, 1-y, 1-z$.

arrangement of the P_2Se_6 units relative to one another is different in the two structures (Tables 2 and 3). The three P−P bonds in **3** are parallel to one another, whereas the P−P bond of the central P_2Se_6 unit in **2** is at an angle to the parallel P−P bonds on either end of the anion. The orientation of the molecular anions relative to one another is also different in the potassium and cesium compounds. In the former, they orient themselves perpendicularly to one another in the *bc* plane, like two overlapping, orthogonal steplike structures, whereas in the latter, they are found to be parallel to one another, forming a pseudolayered structure. The difference in connectivity of the As ions in **2** and **3** may be

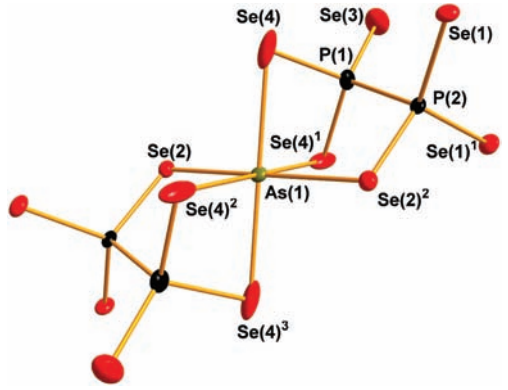

Figure 7. Discrete anionic unit of **4a** with thermal ellipsoids set at 70%. Arsenic sits in a distorted octahedral site with two short and four long bonds. The elongated thermal ellipsoids of Se(4) extend along the As−Se(4) bond axis, most likely indicating the coordinated movement of these atoms around As. Superscript symmetry codes: (1) $x, y, -z$; (2) $-x, 1-y, z$; (3) $-x, 1-y, -z$.

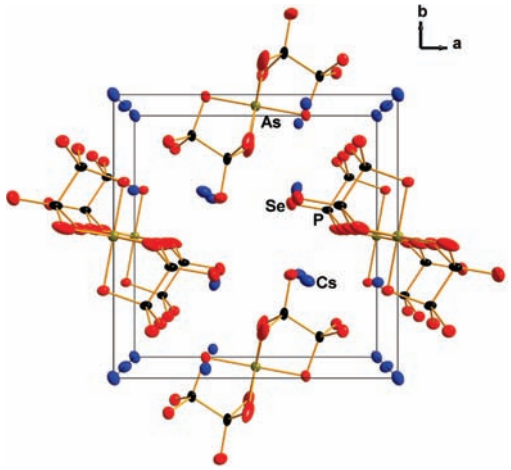

Figure 8. Expanded unit cell of **4a** viewed down the *c* axis. Thermal ellipsoids are set at 90%. A twin law of 180° rotation down the *a* axis was applied to achieve a suitable refinement.

attributed to the larger alkali-metal ion pushing the selenophosphate anions further away from one another, forcing As to chelate to a single $[P_2Se_6]^{4-}$ ligand (Figure 6). Therefore, **3** may be better described as $Cs_6(P_2Se_6)[As(P_2Se_6)]_2$. The pure compound melts congruently at 507 °C and exhibits a sharp absorption at 2.1 eV (Figures S11 and S12 in the Supporting Information). The Raman spectrum of **3** shows a very strong peak at 220 cm^{-1}, attributed to the totally symmetric stretch of $[P_2Se_6]^{4-}$, and all other peaks can again be attributed to various stretches and bends of the anion (Figure S13 in the Supporting Information).

Red crystals of **4a** were first obtained while attempting to make the cesium analogue of **1**. $Cs_5As(P_2Se_6)_2$ crystallizes as well-defined rods in the tetragonal space group $P4_2/m$, and the stoichiometry given by EDS agrees well with the reported values (Figure S14 in the Supporting Information). The structure consists of two $[P_2Se_6]^{4-}$ anions bridged by a single As^{3+} ion that sits in a distorted octahedral environment with two short and four long As−Se bonds of 2.691(2) and 2.732(2) Å, respectively (Figures 7 and 8 and Table 4). The Se atoms [i.e., Se(4)] that have longer bond distances show increased thermal motion along the As−Se bond axis, whereas Se(2) has a relatively spherical thermal ellipsoid.

Table 4. Selected Bond Distances (Å) and Angles (deg) for **4a** at 100(2) K[a]

As(1)−Se(2)	2.691(2)	Se(2)−As(1)−Se(4)	89.94(5)
As(1)−Se(4)	2.732(2)	Se(4)−As(1)−Se(4)	99.76(7)
P(1)−Se(3)	2.105(7)	Se(4)−As(1)−Se(4)	80.24(7)
P(1)−Se(4)	2.216(4)	Se(4)−As(1)−Se(4)	180.0
P(1)−P(2)	2.245(8)	Se(3)−P(1)−Se(4)	115.0(2)
P(2)−Se(1)	2.164(3)	Se(3)−P(1)−Se(4)	115.0(2)
P(2)−Se(2)	2.199(6)	Se(4)−P(1)−Se(4)	105.2(3)
Se(2)−As(1)−Se(2)	180.000(18)	Se(3)−P(1)−P(2)	113.2(3)
Se(2)−As(1)−Se(4)	89.94(5)	Se(4)−P(1)−P(2)	103.6(2)
Se(2)−As(1)−Se(4)	90.06(5)	Se(4)−P(1)−P(2)	103.6(2)
Se(2)−As(1)−Se(4)	90.06(5)	Se(1)−P(2)−Se(1)	114.8(3)
Se(2)−As(1)−Se(4)	89.94(5)	Se(1)−P(2)−Se(2)	112.54(17)
Se(4)−As(1)−Se(4)	180.0	Se(1)−P(2)−Se(2)	112.54(17)
Se(2)−As(1)−Se(4)	89.94(5)	Se(1)−P(2)−P(1)	106.14(19)
Se(2)−As(1)−Se(4)	90.06(5)	Se(1)−P(2)−P(1)	106.14(19)
Se(4)−As(1)−Se(4)	80.24(7)	Se(2)−P(2)−P(1)	103.6(3)
Se(4)−As(1)−Se(4)	99.76(7)	P(2)−Se(2)−As(1)	98.96(16)
Se(2)−As(1)−Se(4)	90.06(5)	P(1)−Se(4)−As(1)	79.32(15)

[a] Symmetry codes: (1) $x, y, -z$; (2) $-x, -y+1, z$; (3) $-x, -y+1, -z$; (4) $-x, -y, -z$; (5) $-x, -y, z$; (6) $-y, x, z-{}^1/_2$; (7) $-y, x, z+{}^1/_2$; (8) $y, -x, -z+{}^1/_2$; (9) $-y, x, -z+{}^1/_2$; (10) $y, -x, z-{}^1/_2$; (11) $y, -x+1, -z+{}^1/_2$; (12) $y, -x+1, z-{}^1/_2$; (13) $y, -x+1, -z-{}^1/_2$; (14) $x, y+1, z$; (15) $-y+1, x, z-{}^1/_2$; (16) $-y+1, x, z+{}^1/_2$; (17) $-y+1, x, -z+{}^1/_2$.

Therefore, coordinated movement of Se(4) around As, resulting in both bonding and nonbonding interactions at any one time, is expected. The pure phase, synthesized by the stoichiometric reaction of Cs_2Se_2, phosphorus, arsenic, and selenium, melts congruently at 416 °C and has a band gap of 2.0 eV (Figures S15−S17 in the Supporting Information). The Raman spectrum of **4a** shows many of the same peaks as the other reported compounds, including a very strong peak at 223 cm^{-1}, which can be attributed to the $[P_2Se_6]^{4-}$ anion (Figure S18 in the Supporting Information).

Attempts to synthesize the sulfur analogues of **1**−**3** resulted in known phases including $K_2P_2S_6$, $Cs_2P_2S_6$, and As_4S_4. However, yellow crystals of **4b** were obtained along with $Cs_4P_2S_{10}$ as an impurity. The sulfur phase was determined to be isostructural to the selenide and, therefore, will not be discussed further. The full characterization can be found in Table 1 and the Supporting Information.

Several compounds have been reported with the same stoichiometry as **4a** and **4b**, although they are not all isostructural. Each of the reported compounds contains a central ion in a distorted octahedral environment (i.e., In^{3+}, P^{3+}, Bi^{3+}) chelated by two $[P_2Se_6]^{4-}$ anions. $Cs_5In(P_2Se_6)_2$[42] is isostructural to **4a** and **4b**; however, $Cs_5P_5Se_{12}$[26] and $Cs_5BiP_4Se_{12}$[19] crystallize in $P\bar{4}$ and $Pmc2_1$, respectively, and exhibit a measurable second-harmonic generation response. It is also interesting to point out that this small molecular anion, $[M(P_4Q_{12})]^{5-}$ (M = As, P, Bi, In), has been isolated only as a cesium salt, which can most likely be attributed to the greater basicity of the larger cation, resulting in a shorter molecular fragment.

Although all reported compounds are molecular salts, the selenides are stable in degassed DMF for more than 1 week but decompose in water and remain insoluble in organic solvents such as *N*-methylformamide, acetonitrile, methanol, and acetone. As mentioned previously, **4b** is stable in degassed DMF for ∼6 h while washing excess flux away, and no noticeable deterioration of the crystals was observed; however, **4b** decomposes in degassed DMF after ∼12 h. The crystals also decompose in water and are insoluble in the above-mentioned organic solvents.

Concluding Remarks

For the first time, compounds containing A/As/P/Q have been synthesized. All are comprised of new discrete molecular arsenic-based chalcophosphate anions that are built from common building blocks that have condensed to form these new anions. The effect of flux basicity and the relative size of the alkali-metal anions are also seen to have an effect on how these structures crystallize differently. These results indicate another possible direction in chalcophosphate and chalcoarsenate synthesis and point toward new and interesting compounds of varying dimensionality that may be possible with other mixed main-group systems.

Acknowledgment. Financial support from the National Science Foundation (Grant DMR-0801855) is gratefully acknowledged.

Supporting Information Available: PXRD patterns, SEM micrographs, EDS results, DTA, Raman spectra, and X-ray crystallographic data in CIF format. This material is available free of charge via the Internet at http://pubs.acs.org.

(42) Chondroudis, K.; Chakrabarty, D.; Axtell, E. A.; Kanatzidis, M. G. *Z. Anorg. Allg. Chem.* **1998**, *624*, 975.